Desalination and Water Treatment
www.deswater.com

doi: 10.1080/19443994.2015.1081836

57 (2016) 16831–16842
August

Taylor & Francis
Taylor & Francis Group

Adsorption kinetics and degradation mechanism study of water persistent insecticide quinalphos: for heterogeneous photocatalysis onto TiO_2

Abhishek Sraw[a], Amrit Pal Toor[a,b,*], R.K. Wanchoo[b]

[a]*Energy Research Centre, Panjab University, Chandigarh 160014, India, Tel. +91 98141 73832; emails: abhisheksraw@gmail.com (A. Sraw), aptoor@yahoo.com (A.P. Toor)*
[b]*Dr. SSB University Institute of Chemical Engineering and Technology, Panjab University, Chandigarh 160014, India, email: wanchoo@pu.ac.in*

Received 11 March 2015; Accepted 4 August 2015

ABSTRACT

The kinetics of adsorption and photodecomposition of the water polluting insecticide quinalphos (QP), in aqueous suspensions of TiO_2 were evaluated under laboratory conditions. Langmuir and Freundlich models were applied to describe the adsorption process and the model proposed by Langmuir–Hinshelwood was used to illustrate the kinetics of the photodecomposition reactions of QP. The adsorption capacity of TiO_2 observed to increase from 7.86 to 20.04 $mg\ g^{-1}$ with the increase in initial QP concentration from 5 to 25 $mg\ L^{-1}$, respectively. About 45.8% adsorption of 20 $mg\ L^{-1}$ QP was observed in just 60 min at pH 6 with 5 $g\ L^{-1}$ TiO_2 loading and 25 ± 1°C temperature. TiO_2 was found to have a maximum adsorption capacity of 23.7 $mg\ g^{-1}$ for QP. Photocatalytic treatment of 200-mL solution (20 $mg\ L^{-1}$) under least harmful UV-A radiations (365 nm/30 $W\ m^{-2}$) with 0.5 $g\ L^{-1}$ TiO_2 loading gives nearly 89.67% degradation in 3 h. The photodecomposition rate of QP was significantly higher at slightly acidic conditions (pH 6). Increasing light intensity from 20 to 35 $W\ m^{-2}$ and aperture to volume ratio of the photoreaction from 0.515 to 1.327 $cm^2\ mL^{-1}$ shows a notable increase in the decomposition rate of QP. Formation of two complex intermediates (m/z 282 and 284) and a few smaller compounds (m/z 104, 108, and 149) were detected by the gas chromatography–mass spectrometry analysis of the reaction sample after 3 h UV irradiation in the presence of TiO_2. These intermediates were further dissociated to simpler hydrocarbons, possibly, by reacting with $^{\cdot}OH$ and $^{\cdot}O$ species.

Keywords: Quinalphos; Titanium dioxide; Catalytic adsorption; Slurry reactor; Photodegradation

1. Introduction

Pesticides are the group of enormously toxic complex organic compounds that are used worldwide for agricultural and household activities. As a consequence of their wide application, pesticides have now become the second largest contaminant in drinking water and therefore have potential toxicity toward living beings [1]. Water contamination is one of the primary sources of human exposure with the toxic compounds. The conventional water treatment processes are not efficient enough to meet the regulatory standards and therefore the development of efficient facilities is the need of the hour [2]. Heterogeneous

---

*Corresponding author.

photocatalysis, as an advanced oxidation process, has received grand attention in degrading such persistent organic compounds and reducing the chemical oxygen demand (COD) in water bodies [3–5]. Illuminated semiconductors have been applied for the remediation of pesticide-contaminated water and in most of the cases, complete mineralization was achieved [6]. Among the long list of semiconductors, titanium dioxide (TiO_2) as a photocatalyst has been widely applied because of its relatively high photocatalytic activity, biological and chemical stability, nonpoisonous nature and long lifespan [7]. The mechanism of the photodegradation by UV-activated TiO_2 is well described by the band gap model given by Bockelmann et al. [8]. It is based on the generation of reactive oxide (·O) and hydroxyl (·OH) radicals, mainly from the adsorbed water and hydroxide ions by the semiconductor [9,10]. These radicals further reacts with the pollutants adsorbed over the surface of the semiconductor to oxidize them into simpler intermediates and ultimately to harmless inorganic products.

Heterogeneous photocatalysis has been studied for the degradation of several toxic and water persistent pesticides including quinalphos (O,O-diethyl O-quinoxalin-2-yl phosphorothioate). Quinalphos (QP) is one of the widely used organophosphate insecticides in Indian agriculture for controlling the caterpillar and scale insects on fruit trees, cotton, vegetables, peanuts, and pest complex on rice [11,12]. It has been found to be a severe irritant for eyes, skin, and respiratory tract, a neurotoxicant and strong inhibitor of acetyl cholinesterase (AChE) [13]. Ranked “moderately hazardous” in World Health Organization’s acute hazard ranking, use of QP is either banned or restricted in most of the nations [14]. However, in India, it is still available in the market by different commercial names such as rolux, captain, flash, ekaphos, and goldlux and applied widely in the agriculture sector.

To prevent the environmental loss caused by such a hazardous chemical, a few researchers had studied the behavior of QP in soil and water. The study conducted by Babu et al. [15] had proved the persistence of QP and its metabolites in Indian soil. Gupta et al. [16] had detected the traces of QP’s metabolites in water even after 80 d of application under natural conditions, which were found to be more toxic than the parent compound. When the aqueous solution of QP was irradiated under very high energy radiations using Xenon arc lamp ($750\ W\ m^{-2}$, 290 nm), it was found to have a half life as long as 20 h [17]. However, UV-B radiations (315–280 nm) are themselves considered the most harmful radiations as they may initiate skin cancer [18,19]. Sidhu and Sud [20] had studied the degradation products of QP (UV 290 nm) by hyphenated technique and quoted the formation of complex intermediates during the process.

Photocatalytic degradation of ethanol-based solution of the QP, using P25-TiO_2 as the catalyst, was studied earlier by Kaur and Sud [12], and they observed that about 40% adsorption of the substrate (QP) over the surface of TiO_2 takes place in just 60 min of the reaction. Since the process of photocatalysis is based upon the surface reactions between the pollutant and the light-activated catalyst, therefore, it is important to study the adsorption behavior of the pollutant on the surface of the catalyst for the effectiveness of the photodegradation for the given pollutant.

The aim of the present study is to: (i) investigate the adsorption behavior of QP over TiO_2 using adsorption models proposed by Langmuir and Freundlich and the effect of various reaction parameters such as catalyst dose, pH, and initial QP concentration on the adsorption; (ii) improve the photocatalytic degradation of QP using P25 TiO_2 by means of least harmful and low energy UV-A radiations (Black-light, florescent tube/367 nm/20 W); (iii) examine the effect of reactor design in terms of area to aperture ratio on the photoactivity of catalyst; and (iv) to characterize the intermediate products, produced by the photocatalytic breakdown of QP and propose the pathway of their breakdown.

2. Material and methods

2.1. Materials

Technical grade insecticide QP (purity 78.2%) was received from Markfed Agro Chemicals, India. Aeroxide P25 (TiO_2) having purity 97%, average particle size of 30 nm and anatase to rutile ratio of (80:20) received as free sample from Evonik, Germany. HCl (LR) and NaOH (essay 97%) were procured from SDFCL, India. Diethyl ether was procured from Merck, India. All chemicals were employed as received without any further treatment. Double-distilled water was used for the preparation of all laboratory solutions.

2.2. Adsorption studies

The experiments of QP adsorption onto TiO_2 were conducted in the absence of light, using a hemispherical glass reactor, having height 8 cm, outer diameter 18.8 cm, and inner base diameter 8 cm, equipped with a digital magnetic stirrer (1,000 rpm). Adsorption experiments were carried out at various concentrations of QP ($5–25\ mg\ L^{-1}$), catalyst loadings

(0.25–1.25 g L^{-1}), and pH (2–10) of the reaction mixture at room temperature (25 ± 1˚C). The pH of 20 mg L^{-1} QP solution was adjusted by either HCl or NaOH before addition of TiO_2. Adsorption isotherms were obtained by treating different concentrations of QP (5–25 mg L^{-1}) using a constant catalyst loading of 0.5 g L^{-1} each time. Aliquots of samples were taken at predetermined time intervals and filtered through a 0.22-μm membrane filtering system (Millipore). The variation in the concentration of adsorbate in the solution was monitored by UV–vis spectrophotometer (Shimadzu UV 2450, Japan) in the wavelength range of 200–800 nm.

2.3. Photodegradation studies

The photodegradation reactions of QP were done in the above-mentioned slurry batch reactor. For UV light irradiation, the reactor was placed in the UV chamber [21,22], fitted with 8 black UV florescent tubes (Philips, 20 W) emitting predominant wavelength of 365 nm, and an exhaust fan was provided on the back wall of the chamber for temperature equilibrium (25 ± 1˚C). The reactor was placed on a digital magnetic stirrer (1,000 rpm) for uniform dispersal of the catalyst, placed on an adjustable stand to attain different distances from UV light source. Effect of various reaction parameters such as catalyst loading (0.25–0.75 g L^{-1}), initial concentration (5–25 mg L^{-1}), pH (4–8), area/volume (A/V) ratio (0.432–1.327 cm^2 m L^{-1}), and light intensity (15–35 W m^{-2}) on the photodegradation of QP have been studied at constant temperature (25 ± 1˚C). At varied time intervals, suitable aliquots (3 mL) were withdrawn from the reaction mixture filtered through 0.22-μm membranes (Millipore) and analyzed using UV–vis spectrophotometer.

2.4. GC–MS analysis

To confirm the breakdown of complex QP into smaller molecules and to identify the metabolites, gas chromatography–mass spectrometry (GC/MS) analysis of the samples has been done at the completion of reaction. The analytical samples were prepared by mixing sample solution and diethyl ether in the ratio 1:2, respectively. The mixture was stirred for 2 h for appropriate mixing and upper layer, i.e. diethyl ether containing QP was extracted thereafter. Appropriate amount of anhydrous sodium sulfate was added to the mixture for the complete removal of water vapors. Finally, the sample was concentrated to 1 mL and analyzed by GC/MS (Thermo GC, TRACE 1300) fitted with a capillary column (TG 5MS, 30 m, 0.25 mm ID, and film thickness of 0.25 μm) attached to a TSQ 8000 mass spectrometer. Helium was used as both the carrier (1 mL min^{-1}) and make-up gas (40 mL min^{-1}). The temperature of injector (splitless mode) was kept at 250˚C, transfer line temperature 280˚C, and oven temperature was programmed from 60˚C (2 min hold) to 300˚C at the rate of 10˚C min^{-1} (5 min hold). To obtain the proposed degradation of byproducts, the peak patterns obtained by the GC/MS were compared to the National Institute of Standards and Technology library.

3. Results and discussion

3.1. Adsorption of QP on TiO_2

3.1.1. Effect of contact time

The adsorption behavior of QP on the surface TiO_2 was measured as a function of the contact time, at different initial QP concentrations from 5 to 25 mg L^{-1}. In Fig. 1, the plot reveals that the adsorption rate was higher at the initial stage of reaction for all concentrations of QP probably due to the availability of larger surface area of TiO_2 at beginning for the adsorption. The increasing contact time increased the adsorption and the equilibrium was observed to attain after 60 min of the contact time in each case.

3.1.2. Effect of initial concentration of QP

While studying the effect of contact time at different initial concentrations of QP, it was also observed that the extent of adsorption decreases with the increase in initial concentration of QP. The percentage QP removal was found to be 78.57% for 5 mg L^{-1} of

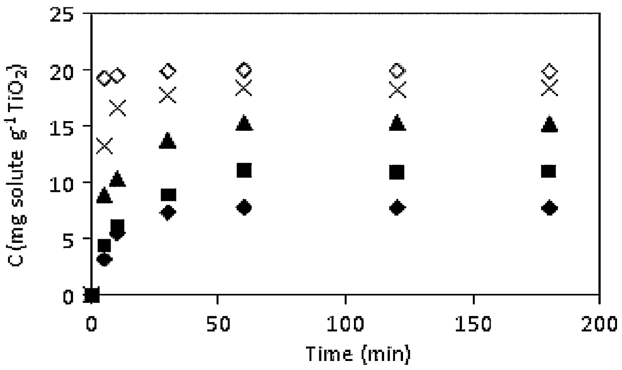

Fig. 1. Effect of contact time on the adsorption equilibrium of various concentrations of QP (TiO_2 loading 0.5 g L^{-1}, QP 200 mL, pH 6, 1,000 rpm); (♦) 5 mg L^{-1}, (■) 10 mg L^{-1}, (▲) 15 mg L^{-1}, (X) 20 mg L^{-1}, (◊) 25 mg L^{-1}.

QP, whereas it was just 40.06% for that of 25 mg L^{-1} QP concentration at constant catalyst loading (0.5 g L^{-1}).

The adsorption ability of a solid surface can be measured by the adsorption isotherm, which is characterized by the amount of solute adsorbed per gram of TiO_2 in conditions of equilibrium. In the present study, the adsorption ability of TiO_2 was calculated by dividing the difference of the initial concentration (C_o) and the equilibrium concentration (C), by the support mass (m) and multiplied by the volume of solution (V) used, in liters, as per the expression given below [23]:

$$C_s = \left[\frac{C_o - C}{m}\right] V \tag{1}$$

A graph was plotted to study the relation between adsorption ability of TiO_2 and the initial concentration of QP (Fig. 2), which reveals that the adsorption is a function of the concentration, and the adsorption capacity increases with the increase in the equilibrium concentration of QP.

The Langmuir and Freundlich adsorption models are most commonly used to study adsorption processes in aqueous solutions as a function of concentration at a given temperature [24]. According to Langmuir's model, adsorption on solid substrate can be described by the following equation [25]:

$$C_s = \frac{K_1 C_{s(m)} C}{1 + K_1 C} \tag{2}$$

where C_s is the adsorption ability of TiO_2, K_1 is Langmuir's equilibrium constant, and $C_{s(m)}$ is the maximum adsorption capacity of the solute on solid substrate. On reciprocating the terms of Eq. (2), we get:

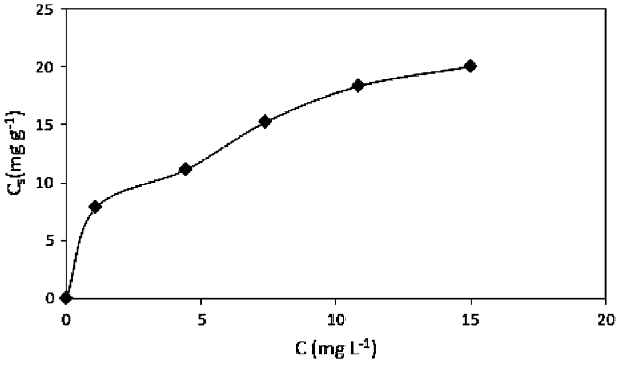

Fig. 2. Equilibrium adsorption isotherms of QP over the surface of TiO_2 at different initial concentrations (5–25 mg L^{-1}) (catalyst loading 0.5 g L^{-1}, pH 6, 1,000 rpm).

$$\frac{1}{C_s} = \frac{1}{K_1 C_{s(m)} C} + \frac{1}{C_{s(m)}} \tag{3}$$

The multiplication of Eq. (3) by C gives the linear form of Eq. (2) as follows:

$$\frac{C}{C_s} = \frac{1}{K_1 C_{s(m)}} + \frac{C}{C_{s(m)}} \tag{4}$$

The plot of C/C_s vs. C has been plotted, and the values of $C_{s(m)}$ and K_1 calculated through the slope and intercept of the straight line were found to be 23.69 mg g^{-1} and 0.331 L mg^{-1}, respectively, (Fig. 3(a)).

According to Freundlich's model, adsorption on solid substrate can be described by the following equation [23]:

$$C_s = K_F C^{1/n} \tag{5}$$

where $1/n$ is the coefficient/degree of linearity; K_F is the Freundlich adsorption constant and C is the equilibrium concentration of the solute. On applying the logarithm to Eq. (5) we get:

$$\ln C_s = \ln K_F + \frac{1}{n} \ln C \tag{6}$$

The values of Freundlich constants, n and K_F were calculated as 2.714 and 7.54 $mg^{(n-1)/n}$ L^{n-1} g^{-1}, respectively, from the slope and intercept of the plot between $\ln C_s$ vs. $\ln C$ (Fig. 3(b)). The values of correlation coefficients (R^2) obtained through Langmuir's and Freundlich's equations indicate that the two models are suitable for evaluating the adsorption of QP over TiO_2.

3.1.3. *Effect of catalyst dose and pH*

To determine the effect of catalyst loading (TiO_2) on the adsorption of QP over TiO_2, the experiments were done at various catalyst doses from 0.25 to 1.0 g L^{-1} under dark conditions at the natural pH of QP solution (pH 6). The observed adsorption trend at a reaction time period of 3 h is given in Table 1. The removal efficiency generally increased with the increase in catalyst loading at a constant temperature, which is because of the availability of more surface area for adsorption due to the increase in the total mass availability [26].

In addition, the influence of solution pH on the adsorption behavior of QP over 0.5 g L^{-1} TiO_2 was

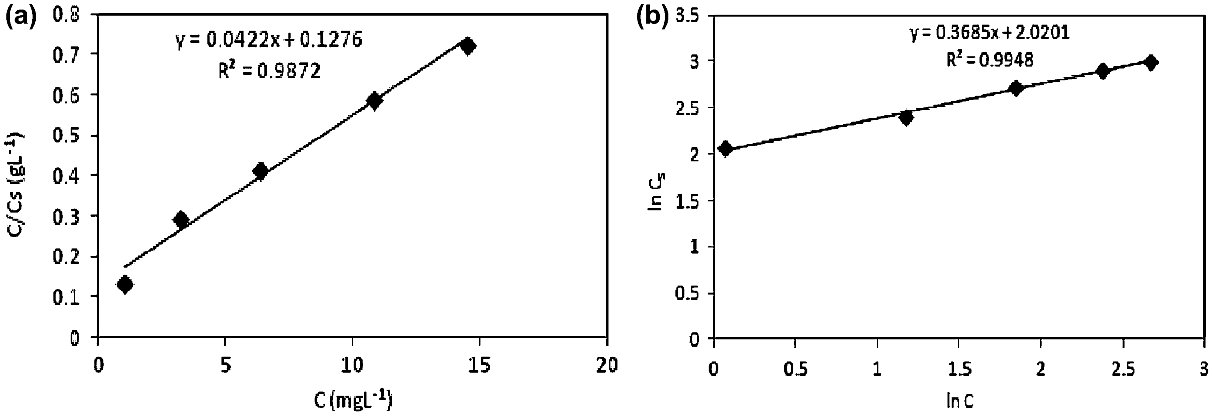

Fig. 3. Linearization of Langmuir (a) and Freundlich's (b) equation for adsorption of QP on TiO_2 at 25°C.

Table 1
Effect of different reaction parameters on adsorption of QP over TiO_2 (Temp. 25 ± 1°C)

Parameters varied	Range	Percentage adsorption
Amount of TiO_2 (g L^{-1})	0.25	38.31
	0.50	45.79
	0.75	52.35
	1.00	64.36
	1.25	63.98
pH	2	37.28
	3	39.45
	4	41.30
	5	44.41
	6	45.79
	7	45.37
	8	44.54
	9	43.65
	10	42.7

also investigated for a time period of 3 h. It was noticed that adsorption of QP increases with the increase in solution pH as we move from acidic to neutral (pH 2–6) conditions, however slight decrease in the adsorption of QP was observed with further increase in the solution pH up to 10 (Table 1). One of the possible reasons behind the lower adsorption at high acidic conditions could be the increased solubility of QP in water as compared to the neutral and basic conditions. Higher solubility may not allow the compound to intact with the surface of TiO_2. Moreover, acidic conditions favor the generation of H^+ ions onto the surface of TiO_2 that has a zero point charge of around 6.3 [27,28] and above this, pH it is negatively charged. Thus, at pH 6, the electrostatic interaction between the positive TiO_2 surface and anionic QP compound takes place and in the absence of UV light radiations, the factor leads to strong adsorption of QP over the surface of TiO_2.

3.2. Photocatalytic degradation study

After studying the adsorption behavior of QP over the surface of TiO_2, degradation studies of QP under least harmful part of UV light (365 nm, 30 W m^{-2}) were carried out. The degradation was negligible under UV light without catalyst at pH 6, whereas about 89.67% decrease in QP concentration was observed when the solution of 20 mg L^{-1} with a catalyst (TiO_2) loading 0.5 g L^{-1} was irradiated under UV light (365 nm) for a period of 3 h.

3.2.1. Kinetics studies

The kinetics of photocatalytic degradation of QP was studied by Langmuir–Hinshelwood (L–H) method. The L–H model was originally developed to quantitatively describe gaseous–solid reactions [29], but later on, it has also been used to describe solid–liquid interactions [30]. According to L–H model, the photocatalytic degradation rate can be expressed as:

$$r = \frac{k_r KC}{1 + KC} \tag{7}$$

where r is the rate of photocatalytic degradation of QP, k_r is the reaction rate constant, K is the equilibrium adsorption constant, and C is the concentration of the substrate at time t, respectively. For dilute concentrations, this equation can be expressed as pseudo-first-order reaction where $k_r K$ can be written as "k_{app}" (apparent rate constant) [23].

To study the dependence of photocatalytic degradation rate of QP at its initial concentration, L–H model as a function of initial concentration was used, and the reaction rate constant and adsorption constant were determined; thus Eq. (7) can be rewritten as:

$$r_o = \frac{k_r K C_o}{1 + K C_o} \tag{8}$$

where r_o is the initial rate of photocatalytic degradation of QP and C_o is the concentration. The inverse of Eq. (8) gives:

$$\frac{1}{r_o} = \frac{1}{k_r} + \frac{1}{k_r K}\frac{1}{C_o} \tag{9}$$

The plot between initial reaction rate and initial concentration is represented in Fig. 4, which shows a linear relationship between the two ($1/r_o$ and $1/C_o$). The values of k_r and K calculated from the intercept and the slope of the straight line ($R^2 = 0.992$) were 1.9723 mg L^{-1} min^{-1} and 0.00632 L mg^{-1}, respectively.

3.2.2. Effect of catalyst loading

To determine the optimal catalyst dosage, experiments were carried out at various amounts of TiO_2 from 0.05 to 0.15 g in 200 mL of an aqueous solution of QP. It was observed that the degradation tends to increase with the increase in catalyst dose from 0.25 to 0.5 g L^{-1} (Fig. 5), however, the degradation rate started decreasing with further increase in the catalyst loading. It is because of the increase in turbidity of the reaction mixture with increasing catalyst loading, which leads to the decrease in light penetration and photoactivity [31]. High catalyst concentration may leads to the aggregation of catalyst particles, thus decreases the number of surface active sites [9]. It also hinder the electronic excitations and hole generation process, therefore, as a result, lesser number of reactive ·OH radicals are available for the degradation of targeted pollutants. The observed optimum catalyst dose (0.5 g L^{-1}) is much lower than that quoted in the literature (1.5 g L^{-1}) for even lesser concentrations (10 mg L^{-1}) of QP [12,20] possibly due to the availability of higher area/volume ratio (0.432–1.327 cm^2 mL^{-1}) of the reactor which allows the light radiations to penetrate the greater depths of reaction solution and photoactivate the catalyst particles more efficiently.

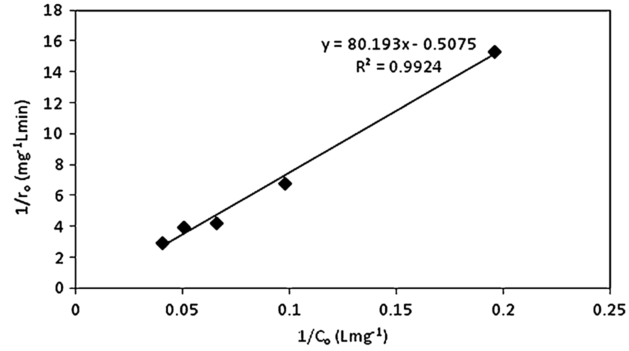

Fig. 4. Plot showing the variation in initial reaction rate with the initial concentration of QP (QP 20 mg L^{-1}, pH 6, UV 30 W m^{-2}, 1,000 rpm).

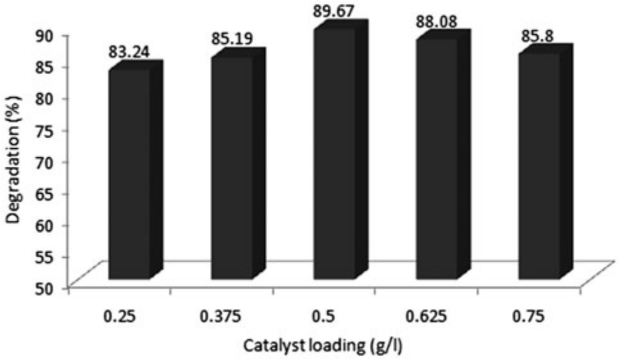

Fig. 5. Effect of different catalyst (TiO_2) loadings on degradation of QP (QP 20 mg L^{-1}, pH 6, UV 30 W m^{-2}, 1,000 rpm).

3.2.3. Effect of pH of the QP solution

The pH of the reaction solution also plays a significant role in photocatalytic process because it affects the solubility of the compounds, surface charge on the catalyst particles, size of the aggregates it forms, and the position of the conductance and valence bands [32]. The effect of pH on the degradation of QP was studied in the pH range 4–8 at constant QP concentration of 20 mg L^{-1} and TiO_2 dose 0.5 g L^{-1}. As shown in Fig. 6, high values of k shows higher degradation of QP at slightly acidic pH, i.e. the initial pH of the stock solution (pH 6); however, pH values higher/lower than pH 6 shows low degradation.

The possible reason behind the observed pattern is the acid–base behavior of TiO_2 surface (zero point charge 6.3) [27,28]. Under UV light conditions, the H^+ ions form reactive $·H_{ads}$ (radicals) by capturing the photogenerated electrons [33], whereas the positive holes serve as oxidation sites to generate ·OH radicals [34]. Both processes collectively act for the effective breakdown of QP.

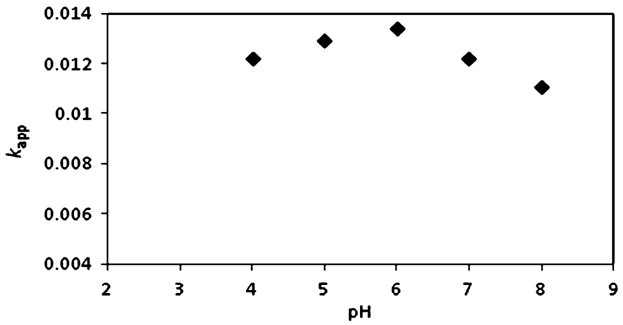

Fig. 6. Effect of varying pH of the reaction mixture on degradation of QP (QP 20 mg L^{-1}, UV 30 W m^{-2}, TiO_2 0.5 mg L^{-1}, 1,000 rpm).

3.2.4. Effect of reactor design (area/aperture ratio)

The degradation in slurry-based photocatalytic reactions depends upon the total amount of light radiations received per unit area of the reaction solution and the depth of the solution to which light can penetrate easily [35]. Thus, an imperative parameter affecting the rate of degradation is the A/V ratio of the reactor setup used for the treatment [36]. With the increase in surface area, the path length of photons entering the solution also increases that will intern enhances the photoactive sites and the formation of ·OH radicals [22].

To study the effect of different A/V ratios of the reactor, degradation of QP was carried out at diverse initial volumes of the solution from 100 to 400 mL, by keeping all other parameters constant. It was observed that as the A/V ratio decreased from 1.327 to 0.515 $cm^2\,mL^{-1}$, the degradation of QP has also decreased from 90.73 to 86.78%. The variation in the rate of reaction at different areas to volume ratio is represented in Fig. 7.

3.2.5. Effect of light intensity

The extent of light absorption by the semiconductor catalyst at a given wavelength depends upon the intensity of the falling light. To study the effect of different light intensities, equal volumes of the solution (200 mL) were kept at different distances from UV light source in order to have intensity values from 20 to 35 W m^{-2}. The area to volume (A/V) ratio was kept constant (0.9188 $cm^2\,mL^{-1}$) for all experiments. In case of shallow pond reactor, the relation between light intensity and the rate of reaction is given by:

$$\frac{k}{k_o} = m\left[\frac{I\left(\frac{A}{V}\right)}{I_o\left(\frac{A}{V}\right)_o}\right]^n \tag{10}$$

where m and n are the experimental constants, k_o is reference rate constant corresponding to reference intensity I_o. At constant A/V ratio, Eq. (10) was converted in to:

$$\frac{k}{k_o} = m\left[\frac{I}{I_o}\right]^n \tag{11}$$

The above equation shows that the rate constant k is directly dependent on the intensity of incident radiations if the A/V ratio is kept constant. The reaction rate constant (k) for QP degradation is directly proportional to the intensity of incident light at constant A/V ratio (Fig. 8).

It is because of the fact that with the increase in light intensity, more photons will be available for excitation and therefore, more electron–hole pairs will be generated over the surface of semiconductor, resulting into increase in the rate of photochemical reaction [37]. The values thus calculated for n and m are found to be 0.726 and 0.953, respectively.

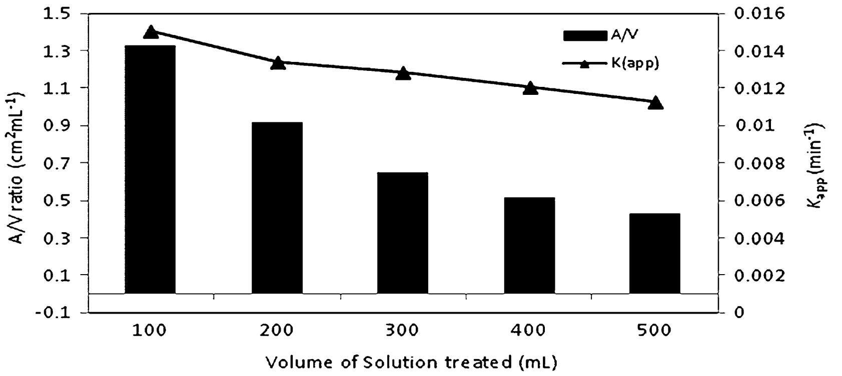

Fig. 7. Effect of A/V ratio of the reactor on degradation of QP (20 mg L^{-1}, pH 6, UV 30 W m^{-2}, 1,000 rpm).

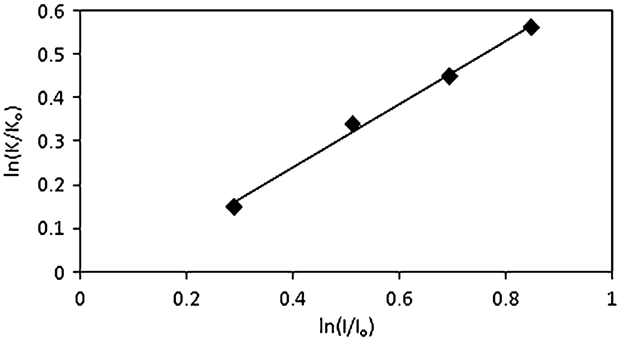

Fig. 8. Effect of different light intensities on degradation of QP at constant A/V ratio (20 mg L^{-1}, pH 6, TiO_2 0.5 g L^{-1}, 1,000 rpm).

4. Mineralization studies

4.1 UV–vis spectra

Samples withdrawn after regular interval of time during the photocatalytic reaction of QP under UV light using TiO_2 were analyzed by the UV–vis absorption spectroscopy. Initial QP gives two representative peaks at 238 and 320 nm as shown in Fig. 9. The resultant graphs at different reaction time periods show gradual decrease in the peak intensities, without formation of any new representative peak, which rules out the formation of any complex byproduct during the degradation of QP.

4.2. COD analysis

The breakdown of complex compound QP was also studied in terms of COD reduction during the photocatalytic treatment under UV light conditions. It was measured as the mass of oxygen required by the organic compounds present per liter of solution for the decay/breakdown and expressed in milligrams per liter (mg L^{-1}). Fig. 10 represents the comparison between the decrease in concentration and percentage COD reduction of QP with reaction time, under UV light conditions. It was observed from the graph that the decrease in COD values took place along with the decrease in concentration of QP with the increasing time of reaction. The reduction in COD of the solution indicates the breakdown of QP to simpler compounds having COD values as low as 8, giving nearly 79% COD reduction in 3 h.

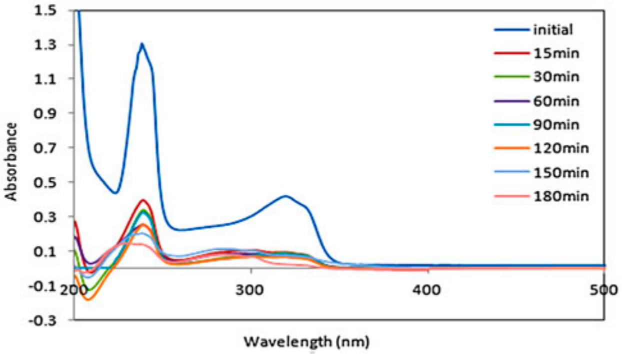

Fig. 9. UV–vis spectra of QP degradation under UV light (TiO_2 0.5 g L^{-1}, 20 mg L^{-1}, pH 6, T 25˚C, UV 30 W m^{-2}).

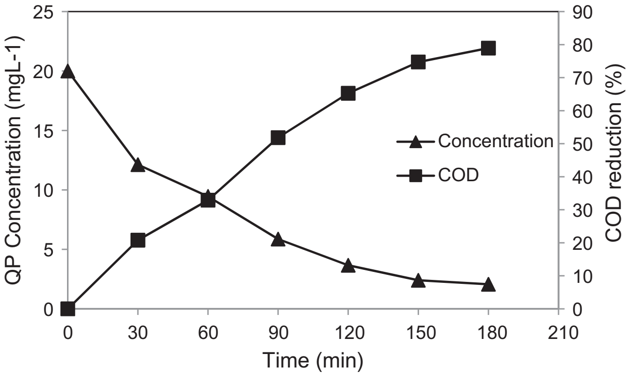

Fig. 10. Plot showing relation between concentration and mineralization of QP in terms of COD reduction with the increase in irradiation time under UV (pH 6, T 25 ± 1˚C, UV 30 W m^{-2}, TiO_2 0.5 g L^{-1}).

4.3. GC–MS analysis

In order to further confirm the UV-assisted photocatalytic degradation of QP and determine the resulting intermediates formed during the process, reaction samples were analyzed by GC–MS. Structures, retention times (R_t), molecular weights (m/z) of the major intermediate compounds, and their breakdown peaks detected by the GC/MS are given in Fig. 11.

The major high intensity peaks were observed at m/z 282 (diethyl 2-quinoxalinyl phosphate) (Fig. 11(d)) and m/z 284 (O-ethyl O-methyl O-quinoxalin-2-yl phosphorothioate) (Fig. 11(e)). Kaur and Sud [12] have reported the intermediate formation mainly in the m/z range of 288–207. Similarly, intermediates with the high m/z values have been detected in the QP degradation in soil and plants [16]. Solar light-assisted degradation of QP has also given the similar range of byproducts [17]. However, in the present study, the detection of comparatively smaller molecules as the major intermediates at m/z 104, 108, and

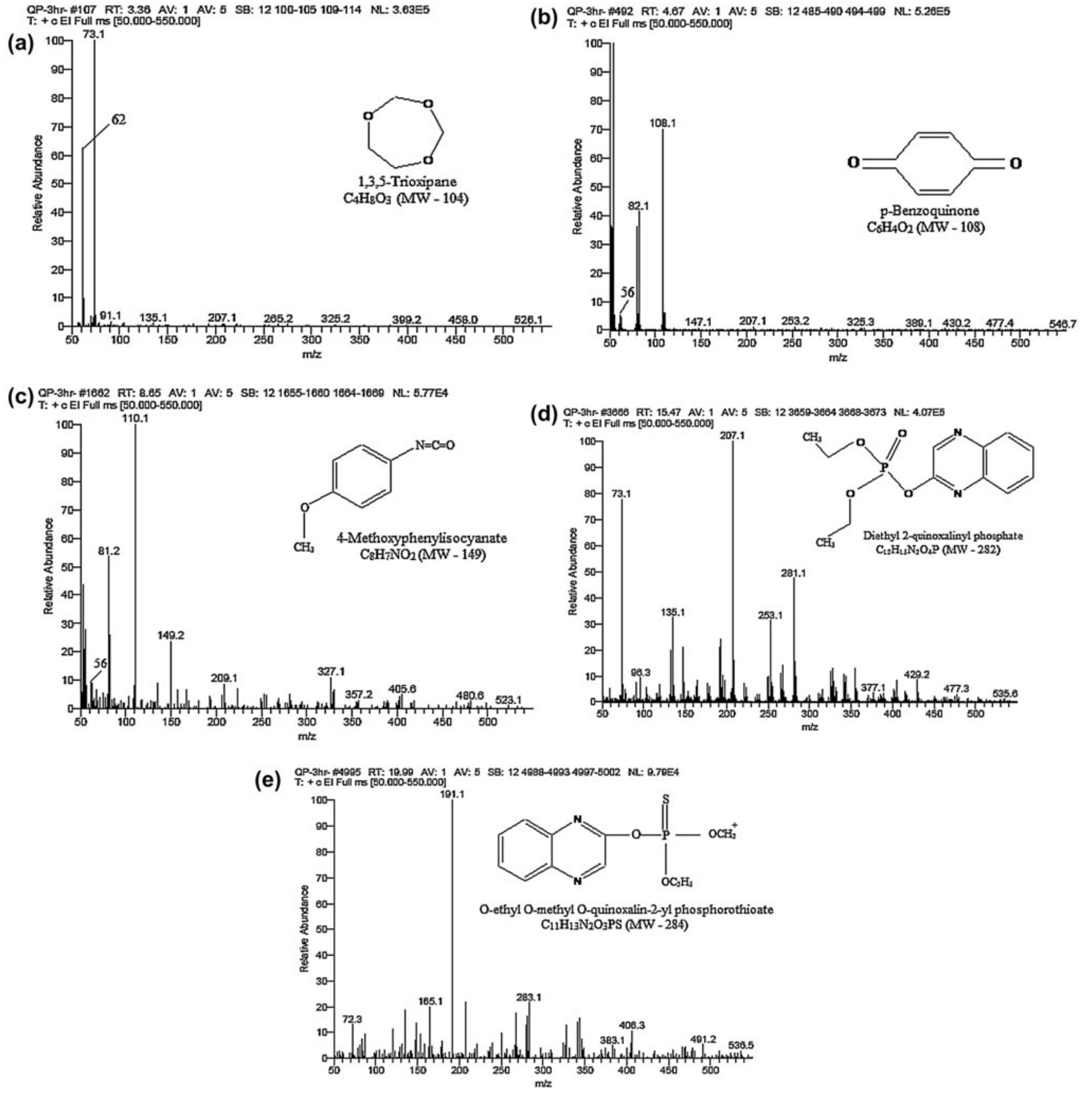

Fig. 11. Mass spectra and proposed structures of detected byproducts of QP, appeared under GC peaks. (a) 1,3,5-trioxipane; (b) p-benzoquinone; (c) 4-methoxyphenylisocyanate; (d) diethyl 2-quinoxalinylphosphate and (e) O-ethyl O-methyl O-quinoxalin-2-yl phosphorothioate.

149 (Fig. 11(a)–(b), respectively) illustrates efficient degradation of QP even with the activation of TiO_2 by UV-A radiations. Further, these intermediates were degraded to simpler linear chain hydrocarbons as detected by GC–MS analysis.

4.4. Proposed probable degradation pathway of the intermediates

Photocatalytic degradation of organic compounds in the presence of TiO_2 is carried out mainly due to the generation of reactive ·O and ·OH free radical species [23]. These radicals further play the leading role in the breakdown of the complex organic materials. In the present analysis, 1,3,5-trioxepane (*m*/*z* 104) was detected as the smallest intermediate at retention time 3.36 min, which readily reduces to propanoate (*m*/*z* 73) by ring cleavage and further to species at *m*/*z* 62 (Fig. 12(a)). Similarly, intermediate p-Benzoquinone (Fig. 12(b)) was detected at retention

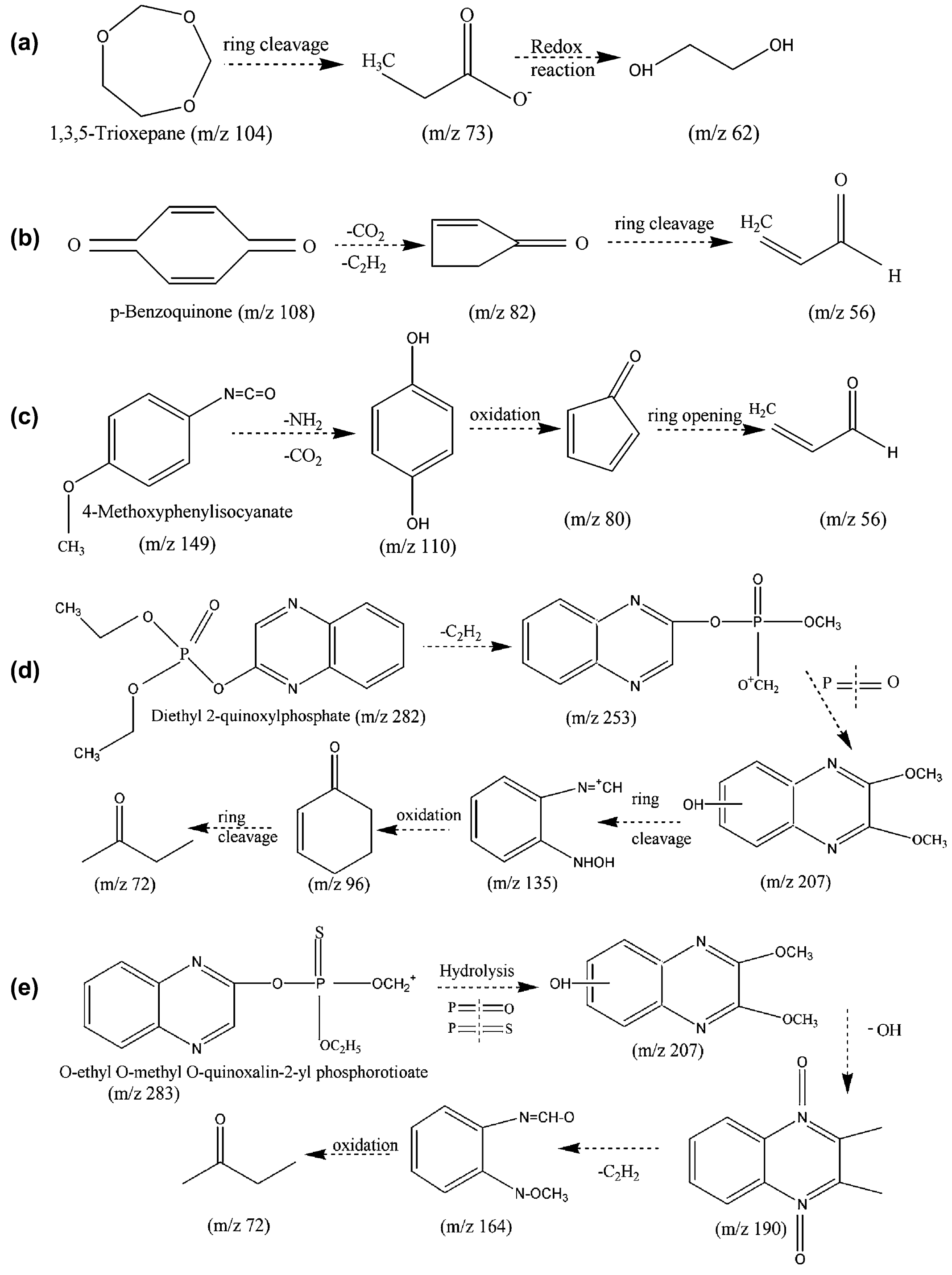

Fig. 12. Possible pathway of the breakdown of intermediates produced by the photodegradation of QP over TiO_2 under UV irradiation: (a) 1,3,5-Trioxepane; (b) p-Benzoquinone; (c) 4-Methoxyphenylisocyanate; (d) Diethyl 2-quinoxylphosphate; and (e) O-ethyl O-methyl O-quinoxalin-2-yl phosphorotioate.

time 4.67 undergoes fragmentation by the removal of $-CO_2$ and $-C_2H_2$ to form species at m/z 82 and 56, respectively. The intermediate at m/z 149 (Fig. 12(c)) having retention time 8.7 breaks to form hydroquinone (m/z 110) by releasing $-NH_2$ and $-CO_2$, which further oxidized to ketonic species at m/z 80, and through ring opening to species at m/z 56. The intermediate at m/z 282 (Fig. 12(d)) having retention time 15.47 gives species at m/z 253 by releasing $-C_2H_2$, which further fragmented to m/z 207 through the breakdown of phosphate bond and thereafter decompose to give species at m/z 135, 96 and straight chain butanone (m/z 72). The principle byproduct at m/z 284 (Fig. 12(e)), formed by the removal of methyl group from QP, undergoes photohydrolysis of the P=S and P=O bond to generate 2,3-dimethoxyquinoxalinol (m/z 207) and 2,3-Dimethylquinoxaline 1,4-dioxide (m/z 190), which further breakdown to form species at m/z 164 by releasing $-C_2H_2$ and simpler molecule butanone (m/z 72).

5. Conclusions

The adsorption study of QP over the surface of TiO_2 shows that at 0.5 g L^{-1} TiO_2 loading and natural pH of QP solution (pH 6), 20 mg L^{-1} of QP gives about 45.8% adsorption in just 60 min at room temperature (25 ± 1˚C). The maximum adsorption capacity of QP over TiO_2 surface was calculated as 23.69 mg g^{-1} using Langmuir adsorption model, whereas the values of K_1 and K_F were found to be 0.331 L mg^{-1} and 7.54 $mg^{(n-1)/n}$ L^{n-1} g^{-1}, respectively, from Langmuir and Freundlich isotherms. Low energy (20 W) and least harmful UV-A (367) radiations were observed to pose very effective TiO_2 activation and delivered 89.67% degradation of 20 mg L^{-1} QP in 3 h with merely 0.5 g L^{-1} catalyst loading at the natural pH of QP solution. Design of the reactor is observed to have a valuable effect on the photoactivity of the catalyst as a gradual decrease in the aperture to volume ratio (A/V) of the photoreactor from 1.327 to 0.515 cm^2 mL^{-1} gives a proportional decrease in the degradation of QP from 90.73 to 86.78%, respectively. GC–MS analysis has detected the formation of several transformation products including two major complexes O-ethyl O-methyl O-quinoxalin-2-yl phosphorothioate and diethyl 2-quinoxalinyl phosphate at m/z 284 and 282, respectively. However, UV–vis spectra and mass spectral interpretation have confirmed the breakdown of these compounds to nontoxic simpler hydrocarbons by the breakdown of P=S/P=O bond after reaction with reactive OH free radicals. Development of a suitable process for direct mineralization of persistent QP under natural sunlight conditions requires further exploration.

Acknowledgments

We would like to acknowledge the following for support and help: the instrumental facilities provided by Central Instrumentation Laboratory (CIL), Punjab University, Chandigarh. Markfed Unit, Mohali (Punjab) for providing the sample of insecticide (QP). Aeroxide (China) for providing free sample of P25-TiO_2.

References

[1] J. Madhavan, P.S.S. Sathish Kumar, S. Anandan, F. Grieser, M.A. Ashokkumar, Sonophotocatalytic degradation of monocrotophos using TiO_2 and Fe^{3+}, J. Hazard. Mater. 177 (2010) 944–949.

[2] T. Oncescu, M.I. Stefan, P. Oancea, Photocatalytic degradation of dichlorvos in aqueous TiO_2 suspensions, Environ. Sci. Pollut. Res. 17 (2010) 1158–1166.

[3] X.Z. Li, Y.G. Zhao, Advanced treatment of dyeing wastewater for reuse, Water Sci. Technol. 39 (1999) 249–255.

[4] D. Robert, S. Malato, Solar photocatalysis, a clean process for water detoxification, Sci. Total Environ. 291 (2002) 85–97.

[5] S. Malato, J. Blanco, A. Vidal, D. Alarcón, M.I. Maldonado, J. Cáceres, W. Gernjak, Applied studies in solar photocatalytic detoxification, an overview, Sol. Energy 75 (2003) 329–336.

[6] M.R. Hoffmann, S.T. Martin, W. Choi, D.W. Bahnemann, Environmental applications of semiconductor photocatalysis, Chem. Rev. 95 (1995) 69–96.

[7] J.H. Lee, M. Kang, S.J. Choung, The preparation of TiO_2 nanometer photocatalyst film by a hydrothermal method and its sterilization performance for *Giardia lamblia*, Water Res. 38 (2004) 713–719.

[8] D. Bockelmann, R. Goslich, D. Banhemann, Solar Thermal Energy Utilization, vol. 6, Springer-Verlag, Berlin, 1992, pp. 398–400.

[9] A. Fujishima, T.N. Rao, D.A. Tryk, Titanium dioxide photocatalysis, J. Photochem. Photobiol. C 1 (2000) 1–21.

[10] A.P. Toor, A. Verma, C.K. Jotshi, P.K. Bajpai, V. Singh, Photocatalytic degradation of Direct Yellow 12 dye using UV/TiO_2 in a shallow pond slurry reactor, Dyes Pigm. 68 (2006) 53–60.

[11] M. Jena, R.C. Dani, S. Rajamani, Effectiveness of insecticides against rice gundhi bug, Oryza 27 (1990) 96–98.

[12] P. Kaur, D. Sud, Photocatalytic degradation of quinalphos in aqueous TiO_2 suspension, Reaction pathway and identification of intermediates by GC/MS, J. Mol. Catal. A-Chem. 365 (2012) 32–38.

[13] K. Vig, D.K. Singh, P.K. Sharma, Endosulfan and quinalphos residues and toxicity to soil microarthropods after repeated applications in a field investigation, J. Environ. Sci. Health B 41 (2006) 681–692.

[14] WHO, The WHO Recommended Classification of Pesticides by Hazard and Guidelines to Classification, World Health Organization, Switzerland, 2009, ISSN 1684–1042.

[15] G.V.A.K. Babu, B.R. Reddy, G. Narasimha, N. Sethunathar, Persistence of quinalphos and occurrence of its primary metabolite in soils, Bull. Environ. Contam. Toxicol. 60 (1998) 724–731.

[16] B. Gupta, M. Rani, R. Kumar, P. Dureja, Decay profile and metabolic pathways of quinalphos in water, soil and plants, Chemosphere 85 (2011) 710–716.

[17] C. Gonçalves, A. Dimou, V. Sakkas, M.F. Alpendurada, T.A. Albanis, Photolytic degradation of quinalphos in natural waters and on soil matrices under simulated solar irradiation, Chemosphere 64 (2006) 1375–1382.

[18] H. Jeffrey, A.J. Fornace, The dark side of light: The damaging effects of UV rays and the protective efforts of MAP kinase signaling in the epidermis, DNA Repair 3 (2004) 567–580.

[19] B.S. Rosenstein, D.L. Mitchell, Action spectra for the induction of pyrimidine(6-4)pyrimidone photoproducts and cyclobutane pyrimidine dimers in normal human skin fibroblasts, Photochem. Photobiol. 45 (1987) 775–780.

[20] P.K. Sidhu, D. Sud, Identification of photocatalytic degradated products of quinalphos by hyphenated technique and degradation pathway, J. Liq. Chromatogr. Related Technol. 37 (2014) 2639–2652.

[21] A. Sraw, R.K. Wanchoo, A.P. Toor, Optimization and kinetic studies for degradation of insecticide monocrotophos using LR grade and P25 TiO_2 under UV/sunlight conditions, Environ. Prog. Sustain. Energy 33 (2014) 1201–1208.

[22] T. Kaur, A.P. Toor, R.K. Wanchoo, Parametric study on degradation of fungicide carbendazim in dilute aqueous solutions using nano TiO_2, Desalin. Water Treat. 54 (2015) 122–131.

[23] J.P.S. Valente, P.M. Padilha, A.O. Florentino, Studies on the adsorption and kinetics of photodegradation of a model compound for heterogeneous photocatalysis onto TiO_2, Chemosphere 64 (2006) 1128–1133.

[24] S. Asuha, X.G. Zhou, S. Zhao, Adsorption of methyl orange and Cr(VI) on mesoporous TiO_2 prepared by hydrothermal method, J. Hazard. Mater. 181 (2010) 204–210.

[25] F.F. Sodré, E. Lenzi, Utilização de modelos físico-químicos de adsorção no estudo do comportamento do cobre em solos argilosos (Applicability of adsorption models to the study of copper behavior in clayey soils), Química Nova 24 (2001) 324–330.

[26] R.R. Kalantary, Y.D. Shahamat, M. Farzadkia, A. Esrafili, H. Asgharnia, Heterogeneous photocatalytic degradation of diazinon in water using nano-TiO_2, Modeling and intermediates, Eur. J. Exp. Biol. 4 (2014) 186–194.

[27] X. Zhu, C. Yuan, Y. Bao, J. Yang, Y. Wu, Photocatalytic degradation of pesticide pyridaben on TiO_2 particles, J. Mol. Catal. A: Chem. 229 (2005) 95–105.

[28] T. Preoanin, N. Kallay, Point of zero charge and surface charge density of TiO_2 in aqueous electrolyte solution as obtained by potentiometric mass titration, Croat. Chem. Acta 1 (2006) 95–106.

[29] C.N. Satterfield, Mass Transfer in Heterogeneous Catalysis, M.I.T. Press, Cambridge, MA, 2004.

[30] D.F. Ollis, Contaminant degradation in water, Environ. Sci. Technol. 19 (1985) 480–484.

[31] N. Daneshvar, D. Salari, A.R. Khataee, Photocatalytic degradation of azo dye acid red 14 in water on ZnO as an alternative catalyst to TiO_2, J. Photochem. Photobiol. A: Chem. 162 (2004) 317–322.

[32] A.P. Toor, A. Verma, C.K. Jotshi, P.K. Bajpai, V. Singh, Photocatalytic degradation of 3,4-dichlorophenol using TiO_2 in a shallow pond slurry reactor, Indian J. Chem. Technol. 12 (2005) 75–81.

[33] B.K. Avasarala, S.R. Tirukkovalluri, S. Bojja, Photocatalytic degradation of monocrotophos pesticide—An endocrine disruptor by magnesium doped titania, J. Hazard. Mater. 186 (2011) 1234–1240.

[34] J. Santhanalakshmi, R. Komalavalli, P. Venkatesan, Photo catalytic degradation of chloropyrifos, endosulphon, imidocloprid and quinolphos by nano crystalline TiO_2—A kinetic study with pH and mass effects, Nanosci. Nanotechnol. 2 (2012) 8–12.

[35] S.K. Sharma, H. Bhunia, P.K. Bajpai, Photocatalytic decolorization kinetics and mineralization of reactive black 5 aqueous solution by UV/TiO_2 nanoparticles, Clean-Soil Air & Water 40 (2012) 1290–1296.

[36] A.P. Toor, A. Verma, V. Singh, C.K. Jotshi, P.K. Bajpai, Treatment of bleaching effluents from the pulp and paper industry by photocatalytic oxidation, Tappi J. 6 (2007) 9–13.

[37] R.S. Dave, Z.F. Thakor, A.R. Patel, Photochemical and photocatalytic reactions of dichlorvos (2,2-dichlorovinyldimethyl phosphate) under UV irradiation, J. Appl. Sci. Environ. Sustain. 6 (2011) 403–409.